Amphiphilic Elastin-Like Block Co-Recombinamers Containing Leucine Zippers: Cooperative Interplay between Both Domains Results in Injectable and Stable Hydrogels
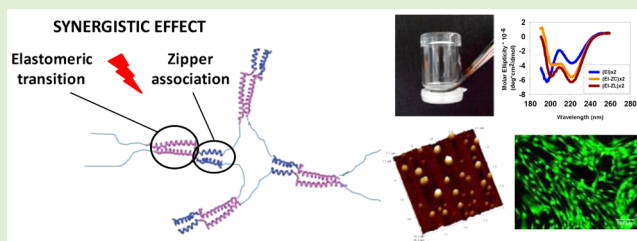
Alicia Fernández-Colino, F. Javier Arias, Matilde Alonso, and J. Carlos Rodríguez-Cabello*

G.I.R. Bioforge, University of Valladolid, CIBER-BBN, Paseo de Belén 11, 47011 Valladolid, Spain

ⓈSupporting Information

ABSTRACT: Many biological processes are regulated by reversible binding events, with these interactions between macromolecules representing the core of dynamic chemistry. As such, any attempt to gain a better understanding of such interactions, which would pave the way to the extrapolation of natural designs to create new advanced systems, is clearly of interest. This work focuses on the development of a leucine zipper-elastin-like recombinamer (ZELR) in order to elucidate the behavior of such domains when coexisting along the same molecule and to engineer reversible, injectable and stable hydrogels. The unique propensity of the Z-moiety selected to dimerize, together with the thermosensitive behavior of the ELR, which has been constructed as a thermosensitive amphiphilic tetrablock, has been engineered into a single recombinant molecule. In this molecular design, the Z-moieties are unable to form a network, while the ELR is below its Tt, thus, guaranteeing the liquid-like state of the system. However, this situation changes rapidly as the temperature increases above Tt, where a stable hydrogel is formed, as demostrated by rheological tests. The inability of the ELR molecule (without Z-domains) to form such a stable hydrogel above Tt clearly points to a positive cooperative effect between these two domains (Z and EL), and no conformational changes in the former are involved, as demonstrated by circular dichroism analysis. AFM shows that Z-motifs seem to induce the aggregation of micelles, which supports the enhanced stability displayed by ZELRs when compared to ELR at the macroscale level. To the best of our knowledge, this is the first time that such an interplay between these two domains has been reported. Furthermore, the cytocompatibility of the resulting hydrogels opens the door to their use in biomedical applications.

■ INTRODUCTION

The ability of many proteins to switch between different oligomerization states is a pivotal tool for controlling their functionality in Nature,[1] with ligand binding, catalytic activity, and a highly ordered organization being just some of the advantages provided by an ability to oligomerize.[1] A rational knowledge of the parameters that determine protein conformation and protein−protein interactions is crucial for the design of artificial bioinspired novel devices that are able to change their aggregated state in an environmentally dependent manner. An ability to undergo such a process in response to a controllable and relevant external stimuli paves the way for the development of nanosensors, molecular transducers, and stimuli-sensitive materials in general.

In this regard, α-helical coiled-coils are known to be responsible for oligomerization in a wide spectrum of proteins.[2] The so-called leucine zippers (Z) are an interesting group of α-helical domains[3] characterized by heptad repeating units designated "abcdefg", where the "a" and "d" positions are occupied by hydrophobic residues such as leucine[4,5] and the "e" and "g" positions are occupied by charged residues.[6] Each coiled-coil domain folds into an amphiphilic α-helix that places the "a" and "d" residues on a hydrophobic face, with hydrophobic interactions driving these helices to associate in a coiled-coil fashion.[7]

Following the school of thought of bioinspiration, which is characterized by the transfer of designs found in Nature to create new and advanced systems in the laboratory, the ability of Z-moieties to oligomerize has been extrapolated to the creation of physical hydrogels.[8−10] The first Z-based self-assembled hydrogel was developed by Petka et al.,[11] and since then, further research in this area has resulted in additional examples being reported.[8,9,12] Despite this, further optimization is still required for real applications. For example, the instability of these hydrogels has always been a handicap, presumably due to the highly hydrophilic environment created by the aqueous media contained within the hydrogel and, in many cases, gel formation has been qualitatively assessed, and with just a few exceptions, quantitative measurement using rheological methods has proved elusive.[8,9] It is worth mentioning that George et al. reported an optimized version of Tirrel's published zipper moieties that was able to form stable zipper-based scaffolds,[10] although additional issues remain unsolved. For example,

gelification takes 3 h, which hampers most of the potential uses of such systems, such as the development of injectable hydrogels.[10] Moreover, the examples of Z-based systems found in the literature tend to focus on a limited number of Z-sequences, which in many cases are artificially designed. As such, further exploration is still required in order to fully exploit the properties that Z-moieties can bring to the field of biomaterials science and nanotechnology.

Taking all this information into account, our working hypothesis is the creation of a novel hybrid molecule, based on Z-domains that are able to form stable, reversible, and injectable hydrogels whose transition between the liquid-like and the gel-like state can be easily controlled by temperature. To this end, Z-domains have been combined with an amphiphilic tetrablock elastin-like recombinamer (ELR) to give a final molecule (ZELR) that combines the properties of the zipper with the thermal responsiveness of the ELR.

ELRs are protein-based materials whose composition is inspired by the primary sequence found in natural elastin.[13] Thus, the amino-acid sequence of ELRs commonly comprises repeats of the (VPGXG) pentapeptide, where X can be any amino acid except proline. ELRs show a reversible phase transition in response to temperature. In an aqueous medium and below a characteristic temperature known as the inverse transition temperature (Tt), the recombinamer chain remains soluble. However, above this Tt, the ELR assembles hydrophobically and adopts a regular, dynamic, and nonrandom structure identified by a succession of β-turns.[14,15]

The amphiphilic tetrablock ELR used here has been reported previously.[16,17] Briefly, it comprises two hydrophilic blocks containing VPGEG pentapeptides along their sequence (in which E stands for glutamic acid) and two thermally sensitive hydrophobic blocks, the pentapeptides of which contain isoleucine as guest residue. The hydrophilic blocks are responsible for water retention within the network of the hydrogel thanks to the ionized state of the carboxyl side chain of E amino acid at neutral pH,[18] whereas the hydrophobic ones are responsible for mediating the physical cross-linking (hydrophobic associations) on increasing the temperature above its characteristic Tt.[16] However, this tetrablock molecule is unable to form a stable hydrogel, losing its integrity in contact with an excess of aqueous medium. The gel swells under these conditions, and finally, at a molecular level, the material goes from a cross-linked hydrogel to a micellar dispersion.[17]

The Z-sequence used in the molecular designed ZELRs developed in this work, known as HLF,[19] belongs to a natural class of human zippers, and the extrapolation of its functionality to the development of new and advanced systems and biomaterials has not been studied to any extent. The HLF sequence belongs to the PAR family of human B-ZIP proteins, which is considered to be the canonical homodimerizing leucine zipper.[19] The choice of this sequence was motivated by the accurate adjustment of this human sequence to the established knowledge of stable dimeric coiled−coil interactions.[19] Moreover, since our understanding of the structure−property relationships in this class of materials is limited, in addition to studying the natural HLF sequence as a means of obtaining such hydrogels, we have also constructed a mutated version in order to shed light on the molecular design principles and to obtain valuable experimental information regarding tailoring of the material's properties.

The main aim of this work is to explore the feasibility of combining Z- and EL-moieties in the same molecule to obtain stable and injectable hydrogels, and to elucidate whether such self-assembled motifs can cooperate when coexisting along the same molecule in order to further understand the behavior of multidomain systems. To this end, two new ZELRs have been designed, produced, and studied, and their gelification behavior, the stability of the hydrogels formed, their structural characteristics at both the nano and the molecular level, and their cytocompatibility are reported in this work.

■ EXPERIMENTAL SECTION

Construction of ELR and ZELR. Gene synthesis was carried out using standard molecular biology protocols. Sequential introduction of the repetitive EL- or Z-polypeptide-coding gene segments to form fusion genes with a fully controlled composition and chain length was carried out using a "recursive directional ligation" (RDL) strategy.[20] To perform such strategy, it is necessary to create coding gene segments flanked at both ends with nonpalindromic restriction sites. Specifically, in the present work, gene segments encoding each monomer were contained in a modified version of the cloning vector pDrive (Qiagen), named as pDAll, which is characterized by the engineering of two inverted Eam 1104 I and one SapI restriction sites in the poly-linker region. Thus, the gene sequence encoding each monomer cloned in pDAll vector is flanked by Eam 1104 I and SapI recognition sites in 5′ termini and Eam 1104 I site at 3′ termini. According to the engineering restriction sites, the restriction type II enzymes Eam 1104 I and SapI were used. The asymmetrical extremities of three nucleotides generated by Sap I are of the same size and orientation as the ones generated by Eam 1104 I endonuclease, which allowed a controlled and sequential concatenation of the gene segments, resulting in a multiblock-coding gene.

The sequences were verified by agarose gel electrophoresis of the restriction fragments generated after enzymatic digestion and automated DNA sequencing. Selected genes were subcloned into a modified pET-25(+) expression vector and then transformed into the E. coli strain BLR(DE3)star (Invitrogen).

ZELR Production and Purification. The purification protocol consisted of sequential rounds of inverse transition cycling (ITC) optimized according to the specific characteristics of each recombinamer.

The soluble fraction obtained at the end of the lysis process of E. coli expression colonies was acidified to pH 4 by addition of diluted hydrochloric acid. The denatured material (acid proteins and DNA) were removed by cold centrifugation at $15000 \times g$ for 30 min. This step was performed at 4 °C to avoid the transition and subsequent aggregation of our recombinamers. The next step consisted on the addition of NaCl 2 M to the soluble fraction, and heating at 42 °C for 1 h. Subsequently, centrifugation at 42 °C was performed, and the insoluble fraction was resuspended by cold ultrapure deionized water. Afterward, cold centrifugation was performed, and the soluble fraction was subjected to two more additional cycles of heating couple with NaCl and cool resuspension. Finally, the recombinamers were subjected to dialysis and lyophilized.

The purity and molecular weight of the recombinamers were routinely determined by sodium dodecyl sulfate polyacrylamide gel electrophoresis (SDS-PAGE) and mass spectrometry (MALDI-TOF/MS). The amino acid composition was further verified by HPLC analysis. NMR (nuclear magnetic resonance) analysis was also carried out in order to ensure the absence of nonproteinaceous organic impurities. In order to characterize the ITT behavior of the recombinamers, DSC experiments were performed using a Mettler Toledo 822e with liquid-nitrogen cooler. The solutions for the DSC experiments were prepared at 5 wt % in an aqueous buffered solution (PBS). A total of 20 μL of the corresponding solution was placed inside a standard 40 μL aluminum pan, which was then sealed hermetically. The heating program for DSC experiments included an initial isothermal stage (5 min at 0 °C for stabilization of the

Table 1. Amino Acid Sequence of the Different Recombinamers[a]

abbreviated name	amino acid sequence	zipper origin
(EI)×2	MESLLP-{[(VPGVG)$_2$-(VPGEG)-(VPGVG)$_2$]$_{10}$[VPGIG]$_{60}$}$_2$-V	–
(EI-ZC)×2	MESLLP-{[(VPGVG)$_2$-(VPGEG)-(VPGVG)$_2$]$_{10}$[VGIPG]$_{60}$-[VGGGGGKENQIAIRASFLEKENSALRQEVADLRKELGKCKNILAKYEAGGGGG]]}$_2$-V	natural (human) Q16534
(EI-ZL)×2	MESLLP-{[(VPGVG)$_2$-(VPGEG)-(VPGVG)$_2$]$_{10}$[VGIPG]$_{60}$-[VGGGGGKENQIAIRASFLEKENSALRQEVADLRKELGKLKNILAKYEAGGGGG]]}$_2$-V	mutated

[a]The natural or mutated feature of the Z-motif of each recombinamer is also indicated. The identifier assigned by UniProtKB data base to the transcription factor that contains the Z-motif used here is also provided. A dash indicates absence of Z-domains. Note that the mutated Z-moiety displays a leucine (L) in the "d" position of the fourth heptad instead of a cysteine (C).

temperature and the state of the recombinamers), followed by heating at 5 °C/min from 0 to 60 °C.

Visualization of the Sol−Gel Behavior. The 15 wt % aqueous solutions of (EI-ZC)×2, (EI-ZL)×2, and (EI)×2 were prepared by dissolving the pure recombinamers in PBS at 4 °C for 16 h. Once the recombinamers had completely dissolved, pictures were taken at 4 °C. Thereafter, the recombinamers were placed at room temperature, and after 2 min, the samples were inverted and pictures were taken.

Stability in an Excess of Aqueous Medium. A solution of each recombinamer at 15 wt % was prepared by dissolving pure lyophilized polymer in aqueous solution (PBS) in glass vials. Once the solution had been obtained, it was incubated at 37 °C for 10 min to ensure hydrogel formation. Immediately afterward, 1.5 mL of PBS was added to the preformed hydrogels. The hydrogels with PBS were placed in a shaker, at 50 rpm and 37 °C and photographs taken at different times (0, 30, 60, and 120 min) in order to monitor the evolution and stability of the hydrogels. After 2 h in the shaker, the erosion of the hydrogels was quantified by spectroscopic methods, measuring the absorbance and by electrophoretic analysis, analyzing the intensity band using KODAK 1D 3.6 software.

Macroscopic Features: Rheology. The mechanical properties of the hydrogels were measured using rheological tests in a controlled stress rheometer (AR2000ex, TA Instruments) equipped with a Peltier plate temperature control.

The conversion of the solution to a gel in the sol−gel process was studied for the three recombinamers (EI)×2, (EI-ZC)×2, and (EI-ZL)×2. A parallel-plate geometry of 20 mm in diameter and a sample volume of 350 μL in PBS was used. The temperature ramp, kinetics of gelation, and the stability over time were carried out at a constant strain of 0.5% and a frequency of 10 Hz. Temperature ramp experiments were performed by heating the sample from 5 to 40 °C. The heating rate was 2.5 °C/min, and the reverse process (cooling) was performed under the same conditions. The kinetics of the gelling process and stability over time was measured at 37 °C.

Circular Dichroism Spectroscopy. Recombinamers were dissolved at a final concentration of 1 mg/mL and were kept overnight at 4 °C. A 1:10 dilution was prepared immediately prior to performing each measurement. The CD spectrum was acquired using a Jasco J-815 150-S spectrometer, using a quartz cuvette with a path length of 0.1 cm. Scans were obtained over the wavelength range 190−260 nm at experimental temperatures of 5 and 37 °C by acquiring points every 0.5 nm using a scan speed of 50 nm/min. Samples were equilibrated for 15 min prior to each measurement. Spectra were corrected by subtracting the corresponding blank solvent readings. The data are expressed molar ellipticity $[\theta]$, which was calculated as follows: ellipticity/[path length (cm) × concentration (mol/L) × 10].

Nanostructured Properties. *Dynamic Light Scattering (DLS).* Solutions of (EI-ZC)×2, (EI-ZL)×2, and (EI)×2 were prepared by dissolving pure, lyophilized products to a concentration of 25 μM in PBS. They were kept at 5 °C for 16 h to allow complete dissolution of the recombinamers, then were filtered using a 0.45 μm PVDF syringe filter. Dynamic light scattering (DLS) measurements were performed using a Zetasizer Nano Series (Malvern Instrumens) equipped with a 10 mW He−Ne laser at a wavelength of 633 nm. Samples were introduced into polystyrene cuvettes and stabilized for 5 min at the desired temperature. Autocorrelation functions were used to obtain the size distribution and polydispersity index.

Atomic Force Microscopy (AFM). Stock solutions of (EI-ZC)×2, (EI-ZL)×2, and (EI)×2 were prepared by dissolving pure, lyophilized products to a concentration of 25 μM in PBS and filtered using a 0.45 μm PVDF syringe filter. They were then kept at 4 °C for 16 h to allow complete dissolution of the proteins. A drop (50 μL) of each sample was deposited onto a clean graphite (HOPG, highly ordered pyrolitic graphite) surface and the dry samples analyzed using a Multimode 8 AFM attached to a Nanoscope V electronics (Bruker) instrument in tapping mode.

Cell Viability. HFF-1 (human foreskin fibroblasts) cell line was used as cell model to test the cytocompatibility of the ZELRs. Fibroblasts are the predominant cell type in the extracellular matrix (ECM) and, thereof, represent one of the main portals of exposition of biomaterials, which justifies the selection of this cell line.

7500 HFF-1 cells were seeded onto 96-well culture plates. The culture medium was removed after 5 h and replaced by 100 μL of the corresponding sterile recombinamer solution in DMEN medium at a concentration of 25 μM. Testing the dispersion of the recombinamers instead of a hydrogel was motivated by current concerns that point to the generation of particulate debris as one of the major causes of failure of any biomaterial implant.[21] In the case of the negative controls, 100 μL of DMEN medium (without any recombinamer) was added.

Live and dead staining (LIVE/DEAD Viability/Cytoxicity Assay Kit, Invitrogen) was used according to the manufacturer's instructions, and fluorescence intensity emission was measured at 425 and 620 nm after excitation at 485 and 525 nm (SpectraMax M5e (Molecular Devices) microplate reader). The fluorescence intensity was converted into a number of HFF-1 cells by using calibration curves obtained with known numbers of HFF-1 cells seeded on 96-well plates 24 h before the measurement (from 1000 to 20000 cells per mL, using 100 μL of DMEN medium). Additionally, cells were visualized with a Nikon eclipse Ti-SR (Japan) fluorescence microscope and images taken. Three independent experiments, each in triplicate, were performed for each recombinamer.

Porous Structure. ZELR hydrogels were dropped into liquid nitrogen and freeze-dried. Imaging of the ZELR hydrogels was performed using a FEI Quanta 200 FEG instrument in low vacuum mode with no prior coating procedures. SEM images were employed to determine hydrogel microstructures.

■ RESULTS AND DISCUSSION

Design and Construction of ZELR and ELR. The amino acid sequences of the different constructs (EI)×2, (EI-ZC)×2, and (EI-ZL)×2 are shown in Table 1. For the sake of simplifying the nomenclature, the HLF motif is referred to in the present work as ZC, whereas ZL- refers to the mutated version of ZC, which is characterized by the presence of leucine (L) in the "d" position of the fourth heptad instead of a cysteine (C) (Table 1). EI- stands for the amphiphilic EL-block in which glutamic acid (E) and isoleucine (I) are the guest residues in the hydrophilic and hydrophobic blocks, respectively. A schematic diagram showing the different domains of (EI)×2, (EI-ZC)×2, and (EI-ZL)×2 is provided in Figure S1 (Supporting Information).

(EI)×2 construction and purification has already been reported.[16] Relative to (EI-ZC)×2 and (EI-ZL)×2, sequential introduction of the repetitive polypeptide-coding gene segments to form fusion genes with a fully controlled composition and chain length was carried out using the recursive directional ligation (RDL) technique.[20] DNA sequencing and restriction mapping analysis showed the correctness of the gene construction process.

ZELR Production and Purification. ZELR purification was successfully carried out using the optimized ITC protocol. To the best of our knowledge, this is the first time that an elastin-zipper based molecule has been purified using such an approach. Although chromatography has been widely applied for the purification of Z-based molecules,[8−10] this technique is expensive and difficult to scale-up. Here, we have successfully made use of the reversible inverse transition of the EL- moieties to purify the whole ZELR hybrid molecule under water-based and mild conditions. Production yields of around 100 mg per liter of bacterial culture were achieved. The final product was characterized by SDS-PAGE electrophoresis (Figure S2), MALDI-TOF mass spectrometry (Figure S3), NMR (Table S1), and amino acid analysis (Table S2), which confirmed the purity and correctness of the biosynthetic process in terms of sequence and molecular mass. DSC experiments were performed in order to check the Tt of the recombinamers (Figure S4).

Visualization of the Sol−Gel Behavior. *Thermogelling Behavior.* Macroscopic observation of the systems clearly indicated that freshly prepared solutions of the three recombinamers, with and without zipper domains, underwent a rapid sol−gel transition upon increasing the temperature above the Tt. Moreover, a liquid-like state was recovered upon lowering the temperature below the Tt (Figure 1).
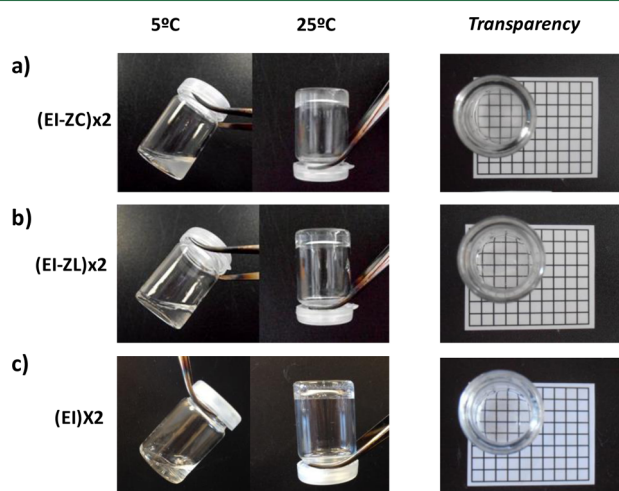
Figure 1. Pictures showing the liquid-like state of the three recombinamers at low temperature and their ability to form hydrogels upon increasing the temperature above the Tt. Visualization of the transparency of (a) (EI-ZC)×2, (b) (EI-ZL)×2, and (c) (EI)×2 hydrogels at 15 wt %.

The Z-motif selected here for the construction of ZELRs is classified as a dimerization sequence as the establishment of higher-order associations is hampered.[6,22] Therefore, when performing our molecular design, we speculated that the formation of a network involving only Z-associations would be hampered by the inclusion of only two HLF motifs per molecule (Table 1), thereby ensuring a liquid-like state of the system when no additional intermolecular contacts mediated by the amphiphilic EL- domains were present, in other words below the Tt of the EL moieties. Such behavior is an essential requirement to achieve an injectable formula. The liquid-like state displayed by ZELR at 5 °C supports the basis of our rational design, with just two dimerizing Z-domains being engineered per molecule to avoid the formation of insoluble networks. Above the Tt of the EL-moieties, it is expected that both kinds of interaction, namely, those mediated by Z- and EL-moieties, would coexist, thus, resulting in the subsequent formation of a hydrogel.

Given the potential utility of these systems in tissue engineering, where in vitro cell cultures require transparent optical properties of hydrogels in order to allow a correct visualization of cell behavior within the scaffold, their transparency properties were checked. As shown in Figure 1, visualization through the corresponding hydrogels was apparent in all cases.

Stability in an Excess of Aqueous Medium. To check the stability in an excess of aqueous medium, PBS was added to preformed 15 wt % hydrogels, as described in the Experimental Section.

The stability of these hydrogels over time clearly differed (Figure 2). Thus, immediately after the addition of PBS, the (EI)×2 hydrogel disaggregated completely, with only a slightly turbid solution remaining (Figure 2c). This contrasts with the behavior displayed by (EI-ZC)×2 and (EI-ZL)×2 hydrogels (Figure 2a,b). Furthermore, (EI-ZC)×2 remained apparently unaltered for at least 2 h (Figure 2d−j), whereas the slight turbidity present in the excess of aqueous medium for the (EI-ZL)×2 hydrogel pointed to a slight disintegration of the system (Figure 2k), although most of the gel remained as such on the bottom of the vial. In all three cases the amount of recombinamer disaggregated from the gel-state was quantified and it was found that, whereas (EI)×2 was completely disaggregated, only 30% of the (EI-ZL)×2 recombinamer was dissolved from the gel state. Furthermore, for (EI-ZC)×2, only 2% of the recombinamer was transferred from the gel to the excess of aqueous medium.

In light of the above, the presence of the Z-motifs clearly improves the stability of the hydrogel when compared to the control. Moreover, when comparing the stability features of both versions of ZELR hydrogels, the gel containing cysteine is more stable than the mutated version containing leucine. As such, we hypothesize that disulfide bond formation is responsible of this increased stability. It is worth noting that the stability of the hydrogel (EI-ZL)×2 is achieved exclusively by means of physical interactions.

Macroscopic Features: Rheological Characterization. *Time Required for Gelation and Stability.* After checking the reversible thermogelling process exhibited by the ZELRs, their stability over time was estimated by rheological methods by applying an isotherm at 37 °C to a sample initially kept at 5 °C. As shown in Figure 3, both ZELRs showed significantly enhanced stability compared to the control ELR (EI)×2. Thus, whereas the (EI)×2 sample undergoes a transient gel state, which lasts only a few minutes, after which the gel state disappears, (EI-ZC)×2 and (EI-ZL)×2 remain in a gel state for the entire time interval studied. Moreover, differences in stability between (EI-ZL)×2 and (EI-ZC)×2 were also detected. Thus, while (EI-ZC)×2 displays a stable modulus (1300 Pa), (EI-ZL)×2 experiences a sustained decrease in its
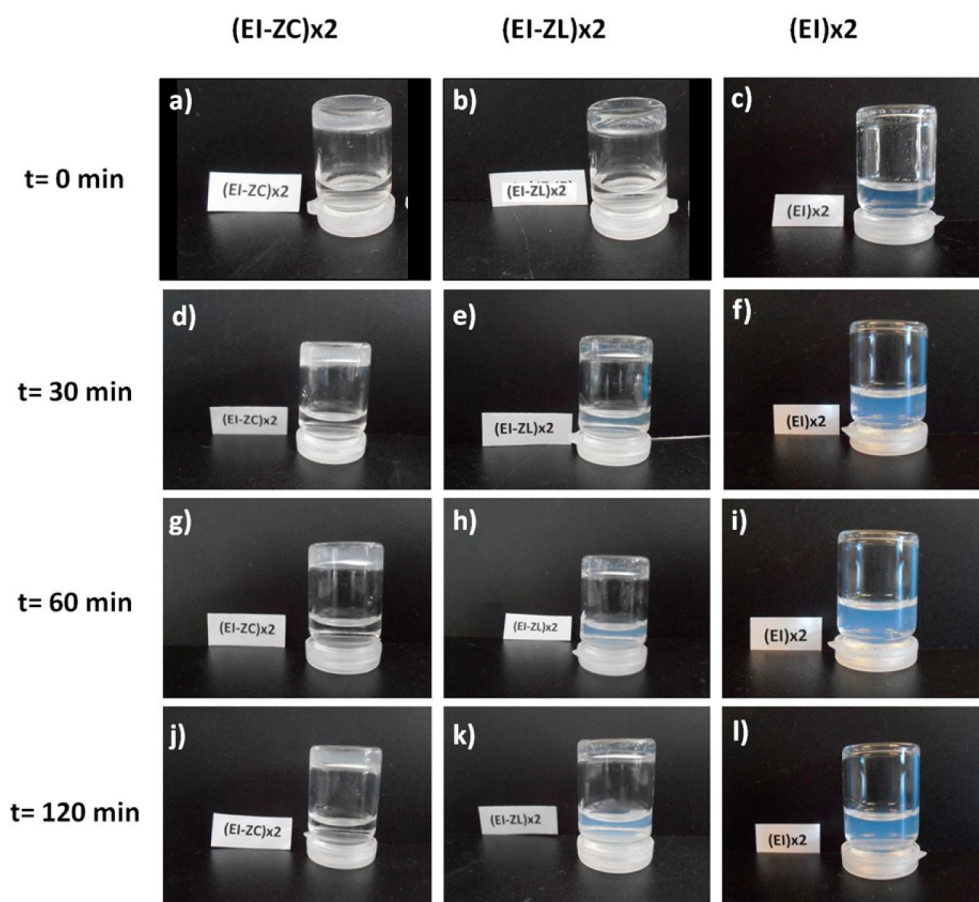
Figure 2. Pictures showing the stability features of (EI-ZC)×2, (EI-ZL)×2, and (EI)×2 after different incubation times at 37 °C while shaking at 50 rpm with an excess of aqueous medium.
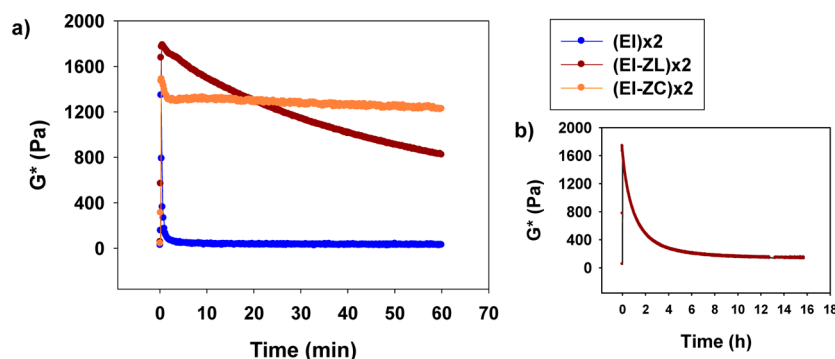

Figure 3. Stability performance of the hydrogels. Isotherms for (EI-ZC)×2, (EI-ZL)×2, and (EI)×2 at 37 °C. (a) Evolution of the complex modulus (G^*) with time for the three recombinamers. (b) Elongation of the isotherm for (EI-ZL)×2 recombinamer until stabilization of the complex modulus is achieved.

mechanical properties until stability is achieved at 150 Pa (Figure 3b). Since the only difference between (EI-ZC)×2 and (EI-ZL)×2 is the substitution of two cysteine residues by two leucines (Table 1), it can be concluded that this substitution is responsible for the differences regarding the stability profile of both recombinamers.

Additionally, the gelation time was less than 1 min for both ZELR solutions (Figure 3). Since the solutions were able to form a gel in a matter of seconds, these materials are potential candidates for use as injectable hydrogels. Moreover, such a short gelation time would presumably avoid diffusion events once the biomaterial is injected, with the consequent

advantages for its application, such as a reduction in the loss of active substances, and consequent improvement in the efficacy of the therapy. The achievement of both features (rapid gelling and stability) represents an important step forward in the development of Z-based hydrogels.

Dependence of Gel State on Temperature. In order to quantify their mechanical properties with regard to temperature, 15 wt % (EI)×2, (EI-ZC)×2, and (EI-ZL)×2 solutions were subjected to a rheological study consisting of heating from 5 to 40 °C at a rate of 2.5 °C/min.

As shown in Figure 4, gel formation occurred for the three samples in the temperature range of 12−18 °C, as is evident
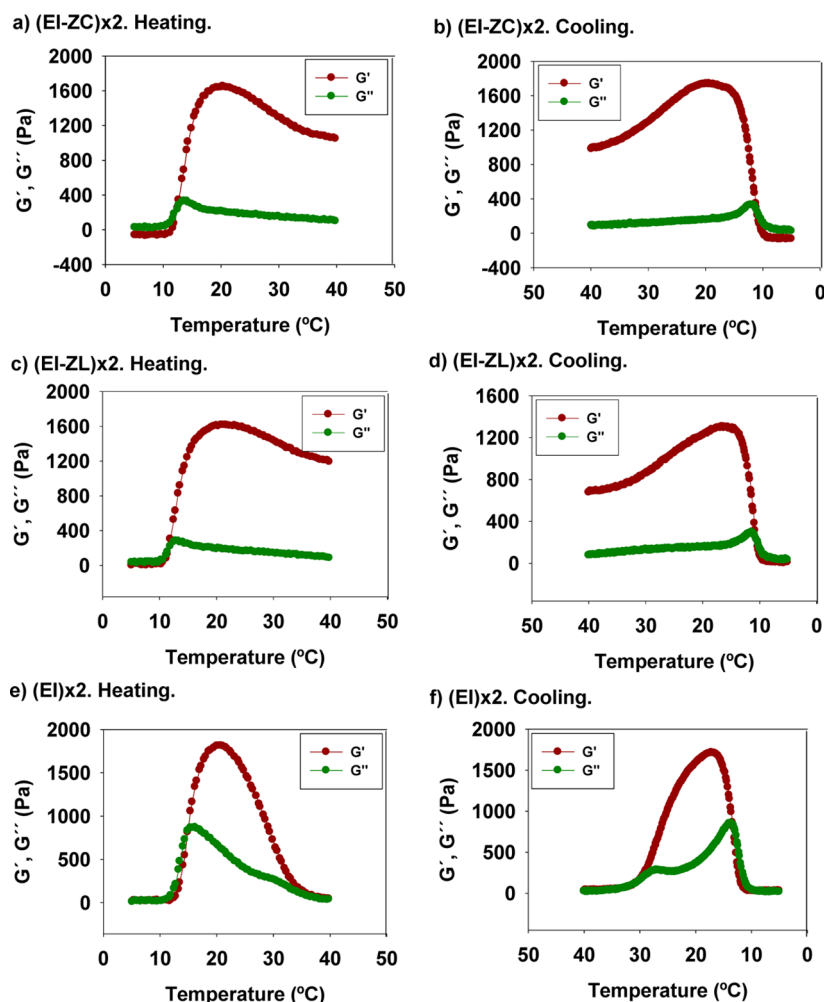
Figure 4. Storage and loss moduli (G', G'') for (EI-ZC)×2, (EI-ZL)×2, and (EI)×2 solutions (15 wt %) as a function of temperature: (a) (EI-ZC)×2 during heating; (b) (EI-ZC)×2 during cooling; (c) (EI-ZL)×2 during heating; (d) (EI-ZL)×2 during cooling; (e) (EI)×2 during heating; (f) (EI)×2 during cooling.

from the $G'-G''$ crossover. However, the gel state for (EI)×2 is not stable over the whole temperature range measured, and although a gel state of 1700 Pa is achieved at 25 °C, at physiological temperature (37 °C) and under these conditions (15 wt % and PBS), the gel state disappears. This behavior contrasts with the behavior exhibited by (EI-ZC)×2 and (EI-ZL)×2, in which the gel state is maintained at 37 °C.

In order to verify the reversibility of the thermogelling process, a cooling ramp was applied from 40 to 5 °C and the resulting mechanical properties monitored. As shown in Figure 4, the thermogelling process is completely reversible. Moreover, the gelation temperature for both (EI-ZC)×2 and (EI-ZL)×2 coincides with that displayed by (EI)×2. These findings suggest that the elastomeric portion exerts an active role in the thermogelling process, with the presence of zipper motifs being essential to achieve final stabilization of the system. Furthermore, (EI-ZC)×2 and (EI-ZL)×2 do not display a gel state at 5 °C, which is indicative that the Z-motif is not able to maintain a network state by itself when the surrounding elastomeric hydrophobic moieties are in a randomly hydrated state. This observation is in accordance with our rational design of the ZELR molecules, into which just two Z-moieties per molecule were engineered in order to promote a liquid-like state of the system at lower temperatures.

Circular Dichroism Spectroscopy. Circular dichroism (CD) spectroscopy analysis was performed to detect whether the previously described rheological observations are related to changes in the conformational state of the molecule and especially to shed light on the conformational state of the Z-domain.

Figure 5 shows CD spectra for (EI)×2, (EI-ZL)×2, and (EI-ZC)×2 at 5 and 37 °C. At 5 °C, an intensely negative band at 197 nm, which is indicative of a predominantly disordered structure, is displayed by (EI)×2. The CD spectra of both (EI-ZC)×2 and (EI-ZL)×2 show a reduced negative band at around 200 nm and an increased negative band at around 220 nm when compared with the spectrum of (EI)×2. These observations suggest that both (EI-ZL)×2 and (EI-ZC)×2 have a higher α-helix content than (EI)×2. At 37 °C, the CD spectrum of (EI)×2 displays a weaker negative signal at 197 nm than that present at 5 °C, whereas the magnitude of the signal at 210 nm increased, thus, suggesting the induction of a type II β-turn conformation with an increase in temperature, as has previously been observed for EL macromolecules.[23,24] In contrast to (EI)×2, which adopted a type II β-turn conformation, the spectra for (EI-ZC)×2 and (EI-ZL)×2 resemble that of an α-helical structure, although with some subtle modifications. Thus, a typical α-helical spectrum is

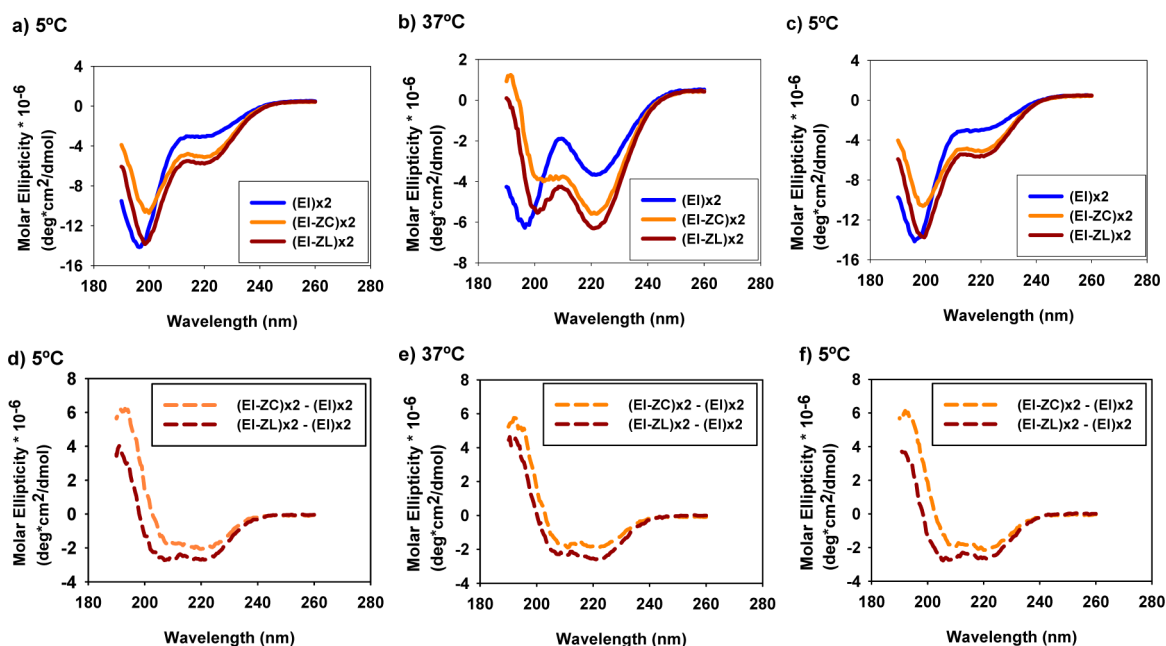**Figure 5.** CD spectra of (EI)×2, (EI-ZL)×2, and (EI-ZC)×2 at different temperatures; Subtraction of CD spectrum for (EI)×2 from those for (EI-ZL)×2 and (EI-ZC)×2, respectively: (a, d) 5 °C; (b, e) 37 °C; (c, f) 5 °C (after heating to 37 °C, to check the reversibility of the conformational changes).
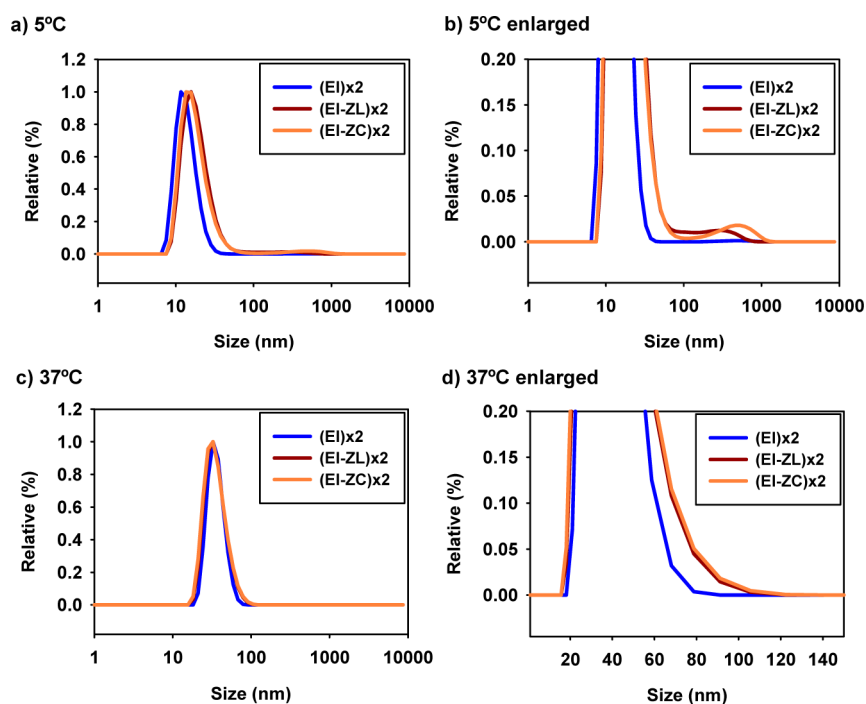

Figure 6. Volume-distribution profiles at 5 °C and at 37 °C for (EI)×2, (EI-ZL)×2, and (EI-ZC)×2.

characterized by a minimum ellipticity at 222 and 208 nm.[25] (EI-ZC)×2 and (EI-ZL)×2 show such minima at 222 and 201 nm. This displacement suggests the presence of a mixture of β-turns and α-helix structures, which agrees with a contribution of both EL- and Z-moieties to the final conformation. The spectrum for (EI)×2 was subtracted from those for (EI-ZC)×2 and (EI-ZL)×2 to more clearly discern the α-helical conformation attributable to the Z-domains.

In order to examine the reversibility of the conformational changes observed upon varying the temperature, the CD spectra of these recombinamers were recorded upon cooling. This showed that the thermally induced conformational changes are completely reversed upon lowering the temperature (Figure 5c–f). These findings are in agreement with the reported rheological data, which also showed a reversible thermogelling behavior (Figure 4). It is noteworthy that the Z-domains remain in an α-helical conformation at both temperatures (5 and 37 °C).

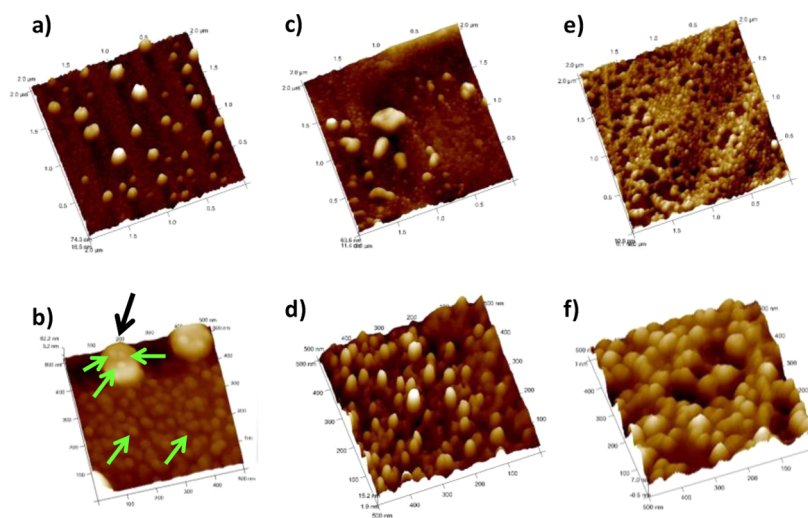As a consequence, the enhanced stability triggered upon raising the temperature (and which is not present in the

Figure 7. Representative AFM images of the nanostructures derived from (EI-ZC)×2, (EI-ZL)×2, and (EI)×2 deposited on an HOPG surface at 37 °C. (a) (EI-ZC)×2 with a scanning window of 2 μm. (b) (EI-ZC)×2 with a scanning window of 0.5 μm. Green arrows mark some representative smaller particles, whereas the black arrow marks a representative largest nanoparticle, apparently formed by fusion of smaller ones. (c) (EI-ZL)×2 with a scanning window of 2 μm. (d) (EI-ZL)×2 with a scanning window of 0.5 μm. (e) (EI)×2 with a scanning window of 2 μm. (f) (EI)×2 with a scanning window of 0.5 μm.

material without Z-domains, namely, (EI)×2) is a consequence of a synergistic effect between both EL- and Z-domains, and no conformational changes in the latter are involved in this increased stability.

Nanostructured Properties. After having studied both the macroscopic and the molecular behavior of these materials, the next step was to determine any differences between the three recombinamers at the nanoscale level.

Dynamic Light Scattering (DLS). Figure 6 shows the particle-size and volume distributions at both 5 and 37 °C for the three recombinamers. In all three cases, nanoparticles are formed upon increasing the temperature from 5 to 37 °C. In particular, (EI)×2 self-assembles into nanoparticles of 35 nm, with a low polydisperisty value of 0.05, thereby indicating a low variation in particle size. Although nanoparticles of a similar size to (EI)×2 are formed by both ZELRs, the polydispersity values indicate a more heterogeneous population. An enlarged view of the volume-distribution profiles confirms these differences (Figure 6d).

It is worth noting that the size distribution of ZELRs is also more heterogeneous than that for (EI)×2 at 5 °C, as can clearly be seen from the enlarged view of the distribution profile (Figure 6b). This observation further supports the notion that the Z-motifs interact at 5 °C and that the liquid-like state is maintained due to the limited number of Z moieties per molecule included in their molecular design, with subsequent importance of this for the achievement of an injectable system.

Atomic Force Microscopy (AFM). AFM was used to visualize the structures detected in the previous DLS studies. As shown in Figure 7, the three recombinamers form spherical nano-particles at 37 °C, although clear differences exist in regard to the homogeneity of the nanoparticle populations. Thus, whereas (EI)×2 self-assembles into a defined and homoge-neous population, (EI-ZC)×2 and (EI-ZL)×2 adopt a more heterogeneous profile, with particle sizes ranging from 25 to 100 nm. Thus, Figure 7b shows that the largest nanoparticle has remnants of the smaller ones, thereby pointing to a possible process of formation of the bigger nanoparticles involving

fusion of the smaller ones. Considering that the only difference between the ZELR molecules and (EI)×2 is the presence of a zipper motif in the former, it can be concluded that this motif plays an important role in the observed fusion of the smaller nanoparticles, giving rise to the more heterogeneous population. These results are in agreement with the DLS measurements. This tendency to higher aggregation displayed by ZELRs when compared to ELRs at the nanoscopic level may be related to the greater stability observed at the macroscopic scale and at higher concentrations. Thus, whereas ELR molecules fail to form a stable hydrogel due to gel disaggregation and micelle dispersion, ZELRs appear to self-assemble into entangled and locked micelles in which the presence of Z-moieties seems to block the disentanglement of bridged micelles.

Cell Viability. Due to the envisaged biomedical applications of these recombinamers, LIVE/dead assays were performed in order to check their cytocompatibility. The quantitative analysis was performed by measuring the corresponding fluorescence emitted by both calcein and EtDH-1 under the three conditions tested, namely, HFF-1 culture treated with (EI-ZC)×2, (EI-ZL)×2, or with any treatment (control), as detailed in the Experimental Section. A one-way analysis of variance (ANOVA) revealed no statistically significant differences in viability between the treatment groups, namely, (EI-ZC)×2, (EI-ZL)×2, and control (without recombinamer).

Microscopic observation corroborated these findings (Figure 8). Furthermore, no morphological differences were observed between the control fibroblasts and the fibroblasts treated with the recombinamers.

Porous Structure. SEM was used to observe the internal structure of the hydrogels. As can be seen from Figure 9, both (EI-ZC)×2 and (EI-ZL)×2 hydrogels showed a highly porous structure, with an important level of interconnection between the pores. Moreover, the diameter of many of the observed pores is around 20 μm, and is thus in the same size range as that displayed by most human cells, with the obvious importance of this fact in view of theirs potential biomedical applications.
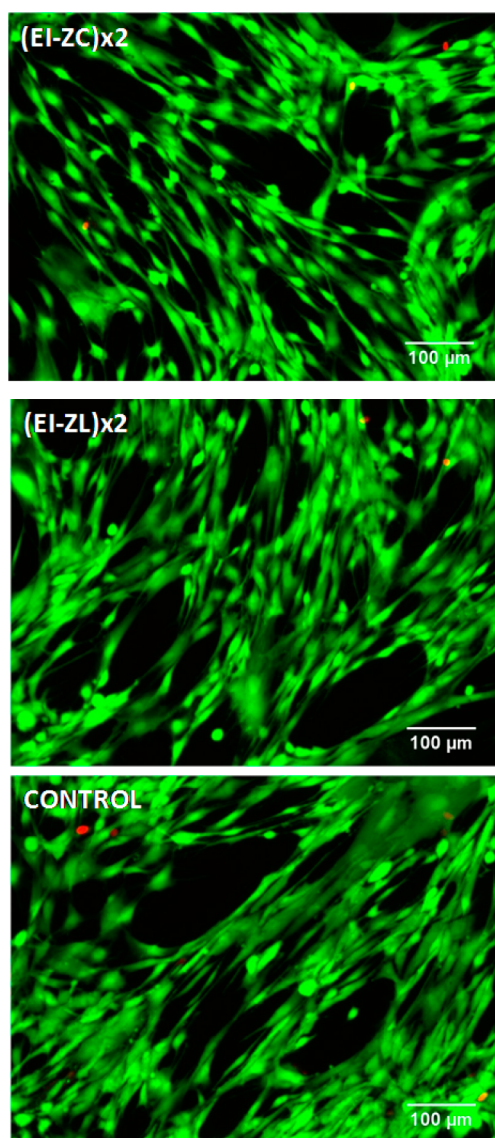
Figure 8. LIVE and DEAD differential staining of HFF-1 cells following culture in TC-PS (tissue culture−polystyrene surface) for 24 h. DMEN medium supplemented with the corresponding recombinamer was used.
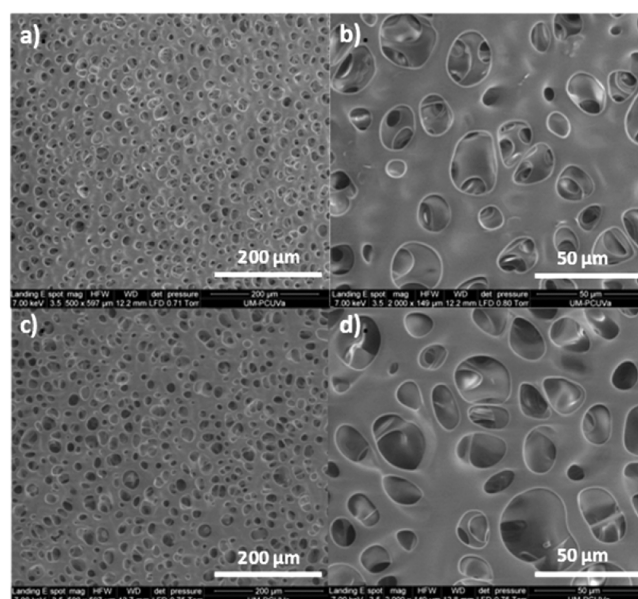

Figure 9. SEM images of (EI-ZC)×2 and ((EI-ZL)×2)×2 hydrogels.

CONCLUSION

Reversible binding events between macromolecules play a crucial role in regulating many biological processes and represent the central axis of dynamic chemistry. Although many examples of the extrapolation of biological designs to the creation of artificial machines can be encountered, a better understanding of the rules that govern the assembly and interactions between the different motifs found in the Nature is required in order to make the most of their potential for designing advanced functional materials.

In this study we report an innovative zipper-elastin-like (ZEL-) molecule in which the connecting blocks between Z-domains have been engineered to form thermally responsive amphiphilic EL tetrablocks. Although some examples of Z-based physical hydrogels have been reported in the literature, in all cases the connecting blocks are essentially spacers with no effect on Z-domain association. As such, the propensity of the selected Z-moiety to dimerize, together with the unique thermosensitive behavior of EL moieties, has been exploited to form a reversible, injectable and stable hydrogel. Furthermore, the stability of this hydrogel points to a positive cooperative effect[26] in which the interaction between the Z- and EL-moieties makes the stability of the assembly as a whole significantly higher than that displayed by the system in which just one of the two motifs is interacting. To the best of our knowledge, this is the first time that such a synergistic effect between both kinds of domains has been reported. In addition, some clues regarding the enhanced stability have been found at the nanoscale level, with the presence of Z-motifs seeming to induce the aggregation of micelles, thereby pointing to a bridged-micelle structure.

In light of the above, and bearing in mind the potential designs offered by recombinant production, the next step will focus on the development of a battery of ZELRs including tailored biofunctionalities in order to use these materials for specific applications in the biological and biomedical fields.

ASSOCIATED CONTENT

Ⓢ Supporting Information

The Supporting Information is available free of charge on the ACS Publications website at DOI: 10.1021/acs.biomac.5b01103.

> A schematic diagram showing the different domains of the recombinamers, SDS-PAGE analysis, MALDI-TOF spectra, amino-acid composition, and DSC analysis for (EI-ZC)×2 and (EI-ZL)×2 (PDF).

AUTHOR INFORMATION

Corresponding Author
*E-mail: roca@bioforge.uva.es.

Notes

ACKNOWLEDGMENTS

636 and MAT2013-42473-R, PRI-PIBAR-2011-1403, and
637 MAT2012-38043), the "Consejeria de Educacion", the JCyL
638 (Projects VA049A11, VA152A12, and VA155A12), the CIBER-
639 BBN, the JCyL, and the Instituto de Salud Carlos III under the
640 Network Center of Regenerative Medicine and Cellular
641 Therapy of Castilla and Leon.

■ REFERENCES

643 (1) Ali, M. H.; Imperiali, B. *Bioorg. Med. Chem.* **2005**, *13*, 5013−5020.
644 (2) Lupas, A. N.; Gruber, M. *Adv. Protein Chem.* **2005**, *70*, 37−78.
645 (3) Krylov, D.; Vinson, C. R. *Encyclopedia of Life Sciences*; John Wiley
646 & Sons, Ltd: New York, 2001.
647 (4) Tripet, B.; Wagschal, K.; Lavigne, P.; Mant, C. T.; Hodges, R. S. *J.*
648 *Mol. Biol.* **2000**, *300*, 377−402.
649 (5) Moitra, J.; Szilak, L.; Krylov, D.; Vinson, C. *Biochemistry* **1997**, *36*,
650 12567−12573.
651 (6) Krylov, D.; Mikhailenko, I.; Vinson, C. *EMBO J.* **1994**, *13*, 2849−
652 2861.
653 (7) Crick, F. *Acta Crystallogr.* **1953**, *6*, 689−697.
654 (8) Mehl, A. F.; Feer, S. P.; Cusimano, J. S. *Biomacromolecules* **2012**,
655 *13*, 1244−1249.
656 (9) Lv, S.; Cao, Y.; Li, H. *Langmuir* **2012**, *28*, 2269−2274.
657 (10) Huang, C. C.; Ravindran, S.; Yin, Z.; George, A. *Biomaterials*
658 **2014**, *35*, 5316−5326.
659 (11) Petka, W. A.; Harden, J. L.; McGrath, K. P.; Wirtz, D.; Tirrell, D.
660 A. *Science* **1998**, *281*, 389−392.
661 (12) Liu, B.; Lewis, A. K.; Shen, W. *Biomacromolecules* **2009**, *10*,
662 3182−3187.
663 (13) Girotti, A.; Fernandez-Colino, A.; Lopez, I. M.; Rodriguez-
664 Cabello, J. C.; Arias, F. J. *Biotechnol. J.* **2011**, *6*, 1174−1186.
665 (14) Urry, D. W. *Angew. Chem., Int. Ed. Engl.* **1993**, *32*, 819−841.
666 (15) Tamburro, A. M.; Guantieri, V.; Pandolfo, L.; Scopa, A.
667 *Biopolymers* **1990**, *29*, 855−870.
668 (16) Martin, L.; Javier Arias, F.; Alonso, M.; Garcia-Arevalo, C.;
669 Rodriguez-Cabello, J. C. *Soft Matter* **2010**, *6*, 1121−1124.
670 (17) Fernandez-Colino, A.; Arias, F. J.; Alonso, M.; Rodriguez-
671 Cabello, J. C. *Biomacromolecules* **2014**, *15*, 3781−3793.
672 (18) Reguera, J.; Fahmi, A.; Moriarty, P.; Girotti, A.; Rodriguez-
673 Cabello, J. C. *J. Am. Chem. Soc.* **2004**, *126*, 13212−13213.
674 (19) Vinson, C.; Myakishev, M.; Acharya, A.; Mir, A. A.; Moll, J. R.;
675 Bonovich, M. *Mol. Cell. Biol.* **2002**, *22*, 6321−6335.
676 (20) Rodriguez-Cabello, J. C.; Girotti, A.; Ribeiro, A.; Arias, F. J. In
677 *Nanotechnology in Regenerative Medicine*; Navarro, M., Planell, J. A.,
678 Eds.; Humana Press: New York, 2012; Vol. *811*, p 319.
679 (21) Kundu, B.; Rajkhowa, R.; Kundu, S. C.; Wang, X. *Adv. Drug*
680 *Delivery Rev.* **2013**, *65*, 457−470.
681 (22) Vinson, C. R.; Hai, T.; Boyd, S. M. *Genes Dev.* **1993**, *7*, 1047−
682 1058.
683 (23) Urry, D. W.; Long, M. M.; Ohnishi, T.; Jacobs, M. *Biochem.*
684 *Biophys. Res. Commun.* **1974**, *61*, 1427−1433.
685 (24) Urry, D. W.; Shaw, R. G.; Prasad, K. U. *Biochem. Biophys. Res.*
686 *Commun.* **1985**, *130*, 50−57.
687 (25) Greenfield, N. J. *Nat. Protoc.* **2007**, *1*, 2876−2890.
688 (26) Hunter, C. A.; Tomas, S. *Chem. Biol. (Oxford, U. K.)* **2003**, *10*,
689 1023−1032.